METAL DUSTING RESEARCH AT ARGONNE NATIONAL LABORATORY*

K. Natesan, Z. Zeng, V. A. Maroni,† W. K. Soppet, and D. L. Rink

Energy Technology Division
†Chemical Technology Division
Argonne National Laboratory
9700 South Cass Avenue
Argonne, Illinois USA

June 2002

Presented at the International Workshop on Metal Dusting, Sept. 26-28, 2001, Argonne National Laboratory, Argonne, IL. and to be published in the Workshop Proceedings.

*Work supported by Office of Industrial Technologies, U.S. Department of Energy, under Contract W-31-109-Eng-38.

METAL DUSTING RESEARCH AT ARGONNE NATIONAL LABORATORY

K. Natesan, Z. Zeng, V. A. Maroni, W. K. Soppet, and D. L. Rink
Argonne National Laboratory
Argonne, IL 60439

ABSTRACT

The deposition of carbon from cabonaceous gaseous environments is prevalent in many chemical and petrochemical processes such as reforming systems, syngas production systems, and iron reduction plants. One of the major consequences of carbon deposition is the degradation of structural materials by a phenomenon known as "metal dusting." There are two major issues of importance in metal dusting. First is formation of carbon and subsequent deposition of carbon on metallic materials. Second is the initiation of metal dusting degradation of the alloy. Details are presented on a research program that is underway at Argonne National Laboratory to study the metal dusting phenomenon from a fundamental scientific base involving laboratory research in simulated process conditions and field testing of materials in actual process environments. The project has participation from the U.S. chemical industry, alloy manufacturers, and the Materials Technology Institute, which serves the chemical process industry.

INTRODUCTION

Production of synthesis gas (mixtures of carbon monoxide and hydrogen) is an important first step in the manufacture of numerous chemicals. The most common process for production of synthesis gas production is steam reforming, where hydrocarbons are converted by reaction with steam over a nickel catalyst at high temperatures. The synthesis gas from the reformer is purified in order to meet the requirements of the downstream process. It can be separated into pure H_2, pure CO, H_2/CO mixtures, etc. Pure CO is required for the production of isocyanates, polycarbonates, and acetic acid, while for example, synthesis of oxo-alcohols requires an H_2/CO mixture with a molar ratio close to 1. By decreasing the steam/carbon ratio and by increasing the outlet temperature of the reformer furnace, great savings in feedstock consumption and in investment can be realized. However, the carbonaceous gases catalyzed by metallic components in these processes result in carbon deposition. Consequences of deposited carbon are the deleterious effect on heat transfer and degradation of structural materials by a phenomenon known as “metal dusting.”

Metal dusting is a catastrophic corrosion phenomenon that leads to the disintegration of structural metals and alloys into dust composed of fine particles of the metal/alloy, carbides, and carbon. Metal dusting occurs at intermediate temperatures of 400-800°C, but this type of corrosion is possible at any temperature at which the carbon activity (a_C) in the gas phase is >>1. Such high carbon activities are prevalent in certain locations in chemical processes such as methanol production, hydrocarbon and ammonia synthesis, hydrogen production, and syngas generation. Even though dusting-related failures have occurred most often in the petroleum and petrochemical industries, and this deterioration has been studied for more than 50 years (Camp et al. 1945; Hoyt and Caughey 1959), its mechanism and driving force are not evident in all cases, and no approach is currently available to mitigate this problem.

A research program is being conducted at Argonne National Laboratory (ANL) to study the metal dusting phenomenon from a fundamental scientific base involving laboratory research in simulated process conditions and field testing of materials in actual process environments with participation from the U.S. chemical industry, alloy manufacturers, and the Materials Technology Institute, which serves the chemical process industry.

Our approach involves characterization, using thermodynamic modeling, of environments prevalent in several process streams in terms of their chemical activities for carbon, oxygen, and other elements. The results are used to assess their chemical potential and temperature windows for metal dusting to initiate and propagate in metallic materials. The thermodynamic assessment would also establish the consequences of equilibrium and nonequilibrium gas chemistries on the metal dusting process.

Bench-scale laboratory experiments are being conducted at ANL with candidate commercial alloys, developmental alloys, and surface-engineered materials, including coatings. Experiments are conducted over a wide range of gas chemistries and temperatures that encompass the environments prevalent in various process systems such as reformers for the production of hydrogen, ammonia, and methanol. Results are used to establish the conditions for onset of metal dusting and to evaluate the influence of alloy chemistry on the occurrence of metal dusting. It is planned to expose candidate commercial, developmental, and surface-engineered alloys in process streams of production plants for hydrogen, methanol, ammonia, and other hydrogen-bearing compounds. The field-exposure results and the laboratory test data will be used to develop performance envelopes for alloys in service with minimum risk of metal dusting.

PRELIMINARY CALCULATIONS

Gas Phase Reactions

Chemical process environments were characterized by computer modeling of gas-phase reactions under both equilibrium and nonequilibrium conditions. Calculations were made to evaluate carbon activities (a_C) for different gas mixtures as a function of temperature at atmospheric pressure (14.7 psia) and at plant system pressures. Chemical compositions are listed in Table 1 for seven gas mixtures, which include the reformer streams and laboratory simulation environments. The carbon deposition process can be influenced by two possible reactions, as follows:

$$CO(g) + H_2(g) = C + H_2O(g) \quad (1)$$

$$2CO(g) = C + CO_2(g) \quad (2)$$

Since the gas composition is maintained fairly constant during the passage through the waste-heat boiler for the reformer streams, either Reaction 1 or Reaction 2 may dictate the a_C at different temperatures. If it is dictated by Reaction 1, a_C will be directly proportional to the H_2 and CO partial pressures and inversely proportional to the H_2O partial pressure. On the other hand, if a_C is dictated by Reaction 2, then it will be directly proportional to square of the CO partial pressure and inversely proportional to the CO_2 partial pressure. In addition, if gas-phase equilibrium does prevail, albeit at high temperatures and/or for long residence times, then the calculated a_C value will be the same (i.e., irrespective of Reaction 1 or 2) since thermodynamically the gas composition will adjust to give the most stable (lowest free energy)

composition. Therefore, a_C was calculated as a function of temperature (496°C or 925°F to the maximum test temperatures and 1 atm to the maximum test pressures) for the seven gas mixtures assuming Reaction 1 or 2 is dominant and the gas phase is in assumption of thermodynamic equilibrium.

Carbon Activity Calculations

Table 2 lists a_C values calculated for the seven gas mixtures (Table 1) at 593°C (1100°F) and 704°C (1300°F), based on whether Reaction 1 or 2 was dominant or equilibrium among different gas species prevailed. Figures 1-3 show plots of a_C as a function of temperature for the three reformer outlet-gas mixtures listed in Table 1. Figure 1 shows six curves for Gas Mixture 1, as follows:

Case 1: Reaction 1 dominant, P = 1 atm (14.7 psia)

Case 2: Reaction 1 dominant, P = 37 atm (543, psia)

Case 3: Reaction 2 dominant, P = 1 atm (14.7 psia)

Case 4: Reaction 2 dominant, P = 37 atm (543 psia)

Case 5: Equilibrium condition, 1 atm (14.7 psia)

Case 6: Equilibrium condition, P = 1 atm (543 psia)

Similar curves are shown in Fig. 2 for Gas Mixture 2, and in Fig. 3 for Gas Mixture 3. The maximum pressures for Gas Mixtures 2 and 3 are 15 atm (215 psia) and 32 atm (470 psia), respectively.

Table 1 Chemical compositions of gas mixtures relevant for metal dusting study.

	Composition in mole %						
Gas species	**Gas 1**	**Gas 2**	**Gas 3**	**Gas 4**	**Gas 5**	**Gas 6**	**Gas 7**
CH_4	4.1	1.1	0.2	-	-	-	-
CO	7.2	18	8.4	17.5	17.6	12.7	70.0
CO_2	5.7	5.6	5	8.3	8.3	10.1	4.0
H_2	43.8	52	36.3	74.2	72.2	77.2	25.25
H_2O	39.2	23	35	0	1.96	0	0.007
N_2	-	-	15	-	-	-	-
Ar	-	-	0.1	-	-	-	-

Gases 1, 2,and 3: Reformer outlet gases. Gases 4, 5, and 6: Used in ANL experiments. Gas 7: Used in Special Metals Program.

Table 2 Carbon activity values at 593°C (1100°F) and 704°C (1300°F) based on reactions 1, 2, and equilibrium, calculated for gas mixtures listed in Table 1.

	593°C (1100°F)			704°C (1300°F)		
Gas #	**Rxn 1**	**Rxn 2**	**Eqm**	**Rxn 1**	**Rxn 2**	**Eqm**
1	0.4	1.2	0.3	0.05	0.08	0.09
2	2.0	7.9	0.7	0.24	0.53	0.25

3	0.4	1.9	0.2	0.05	0.13	0.04
4	∞	5.0	1.3	∞	0.34	0.8
5	32.3	5.0	1.2	3.8	0.34	0.7
6	∞	2.2	0.01	∞	0.15	0.02
7	117.4	165.4	32.6	13.8	11.1	6.2

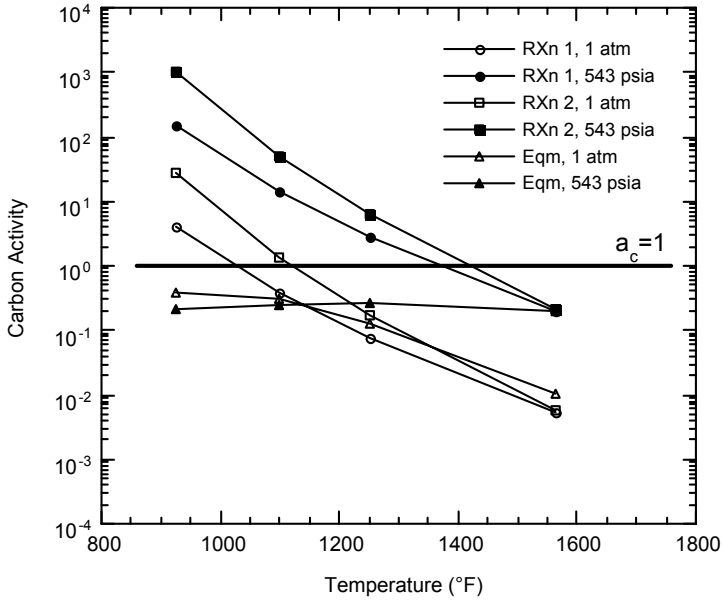

Figure 1 Carbon activity curves calculated as a function of temperature for Gas Mixture 1.

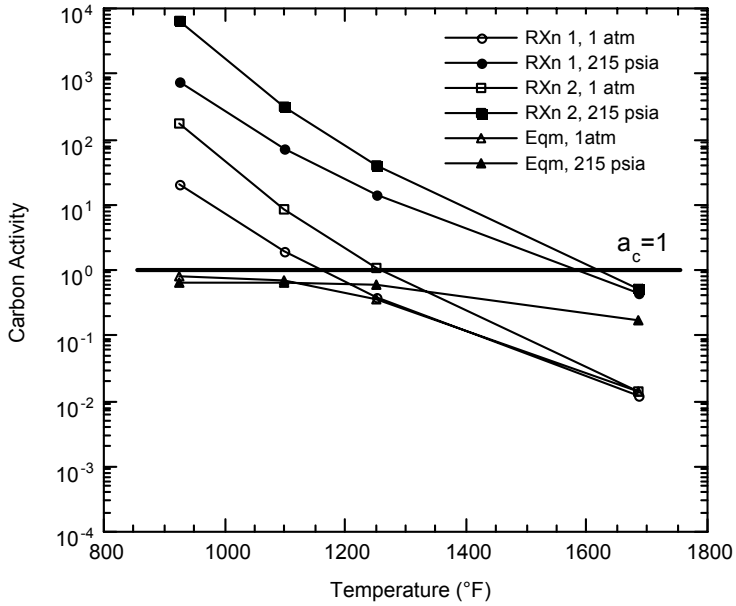

Figure 2 Carbon activity curves calculated as a function of temperature for Gas Mixture 2.

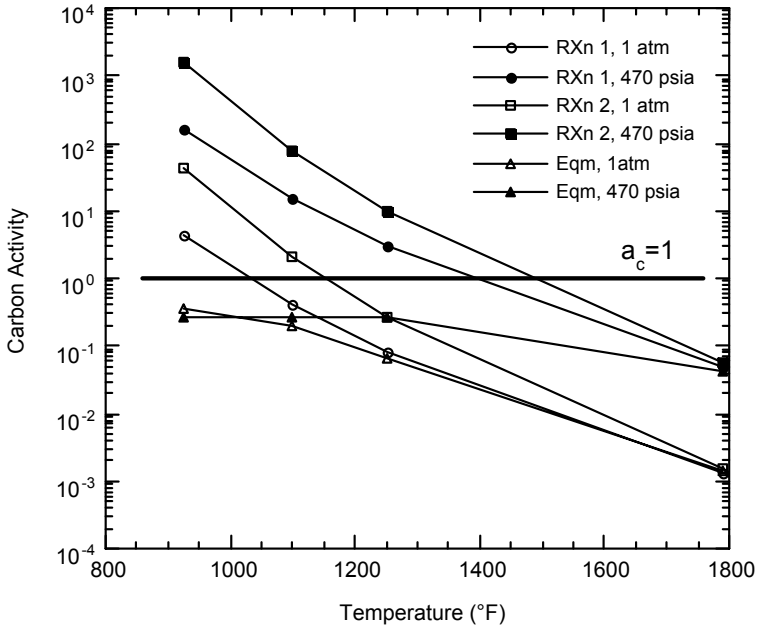

Figure 3 Carbon activity curves calculated as a function of temperature for Gas Mixture 3.

The implications of the carbon activity calculations are as follows:

1. Under nonequilibrium conditions, Reaction 1 control at 1 atm pressure results in the lowest a_C for all reformer gas mixtures (Gases 1-3). Even under these conditions, a_C is 1 or higher at temperatures below ≈565°C (≈1050°F) for Gas Mixtures 1 and 3 and below ≈621°C (≈1150°F) for Gas Mixture 2. At 496°C (925°F), a_C is ≈4 for Gas Mixtures 1 and 3 and ≈20 for Gas Mixture 2. These a_C values can result in carbon deposition at 496°C (925°F) and may lead to metal dusting of several alloys, depending on the incubation time and alloy composition.

2. Reaction 2 control always results in higher a_C. This trend is evident at all temperatures and pressures for the present calculations. Furthermore, this trend is independent of the gas mixture used in the calculation. The differences in the absolute value of a_C established under Reaction 1 versus Reaction 2 control can be used to assess the role of these reactions in carbon deposition and associated metal dusting. For example, if an experiment is run in Gas Mixture 1 at 579°C (1075°F) and 1 atm pressure, Reaction 1 control (with a_C of ≈0.6) would result in no carbon deposition whereas Reaction 2 control (with a_C of ≈3) would result in carbon deposition.

3. Increased system pressure increases the a_C calculated for both reactions, irrespective of the gas composition. The carbon activity increases in direct proportion to the total pressure, and the value could be extremely large at lower temperatures. Furthermore, the effect of increased pressure is to widen the temperature window in which $a_C >> 1$. For example, in Gas Mixture 1 with Reaction 1 control, an increase in pressure from 1 atm (14.7 psia) to 37 atm (543 psia) increases the temperature window with $a_C > 1$ from 427-565°C (800-1050°F) to 427-732°C (800-1350°F). This assumes that temperatures <427°C (<800°F) is too low to initiate metal dusting degradation, even though a_C is high.

4. Calculations also indicate that under equilibrium conditions, all reformer gas mixtures exhibit a_C <1 (even at high pressures); therefore, no deposit of carbon and associated metal dusting should occur. Since carbon deposition and metal dusting of structural alloys are widely observed in reformer systems, the gas mixtures in these systems are not really in equilibrium, and a_C is established by individual reactions and is dictated by the reformer effluent gas composition.

5. Calculations further show that experiments need to be conducted under nonequilibrium gas chemistry to deposit carbon (coke) and also allow sufficient incubation time for metal dusting to initiate.

6. For gas mixtures 4 and 5, a_C will be >1 if Reaction 1 is dominant. If Reaction 2 is dominant, a_C will be >1 at 593°C (1100°F) and <1 at 704°C (1300°F).

Results from these analyses were used to select gas compositions and temperatures for the experimental effort on metal dusting of structural alloys.

EXPERIMENTAL PROGRAM

Equipment Description

In all, five experimental systems were used in the metal dusting experiments. Two existing systems at ANL were modified to accommodate the requirements of the program. Each of the modified systems consisted of a horizontal, tubular, high-temperature furnace capable of operation up to 900°C. The reaction chamber, with gas inlet/outlet fittings, fabricated from quartz was positioned within the furnace chamber. A chromel-alumel thermocouple, inserted from one end of the reaction chamber, was used to monitor the specimen temperature. Specimens were suspended from quartz rods held on the top of a high-purity alumina boat. The specimens and the boat were positioned in the constant-temperature section of the reaction chamber. High-purity gases such as CO, CO_2, CH_4, and H_2 were procured and piped into the reaction chamber through flow meters to obtain the desired composition. In some experiments, H_2 gas was bubbled through a water bath to saturate the H_2 with water prior to entering the reaction chamber.

While the two systems described above enabled study of the key variables in metal dusting research, additional facilities were needed for long-term testing of metallic alloys, surface-engineered materials, and coatings, especially in environments that contained a large H_2O content. For this purpose, three new systems were designed and assembled in a metal dusting research laboratory. Figure 4 shows a schematic diagram for the three test facilities. The three test fixtures were positioned horizontally on a laboratory bench top in a staggered linear arrangement with a common gas supply. Each test fixture consists of a quartz retort chamber (74-cm length, 5-cm OD, 0.32-cm thick), which was centered in a 30-cm diameter resistive heating furnace. A Barber-Coleman Model 560 three-mode controller was used to control the furnace temperature. Type 316 stainless steel (SS) flange caps with an O-ring seal closed the ends of the quartz retort tube. The flange caps provided port fittings for the gas flow, steam/vapor preheater, and ceramic thermowells used for specimen temperature measurements.

The gas that flowed through the retort chamber had various ratios of H_2, CH_4, CO, CO_2, and steam/water vapor. Gases from the low-pressure manifold lines were supplied to respective individual Brooks model 5850S computer-controlled digital mass flow controller (DMFC)

valves.

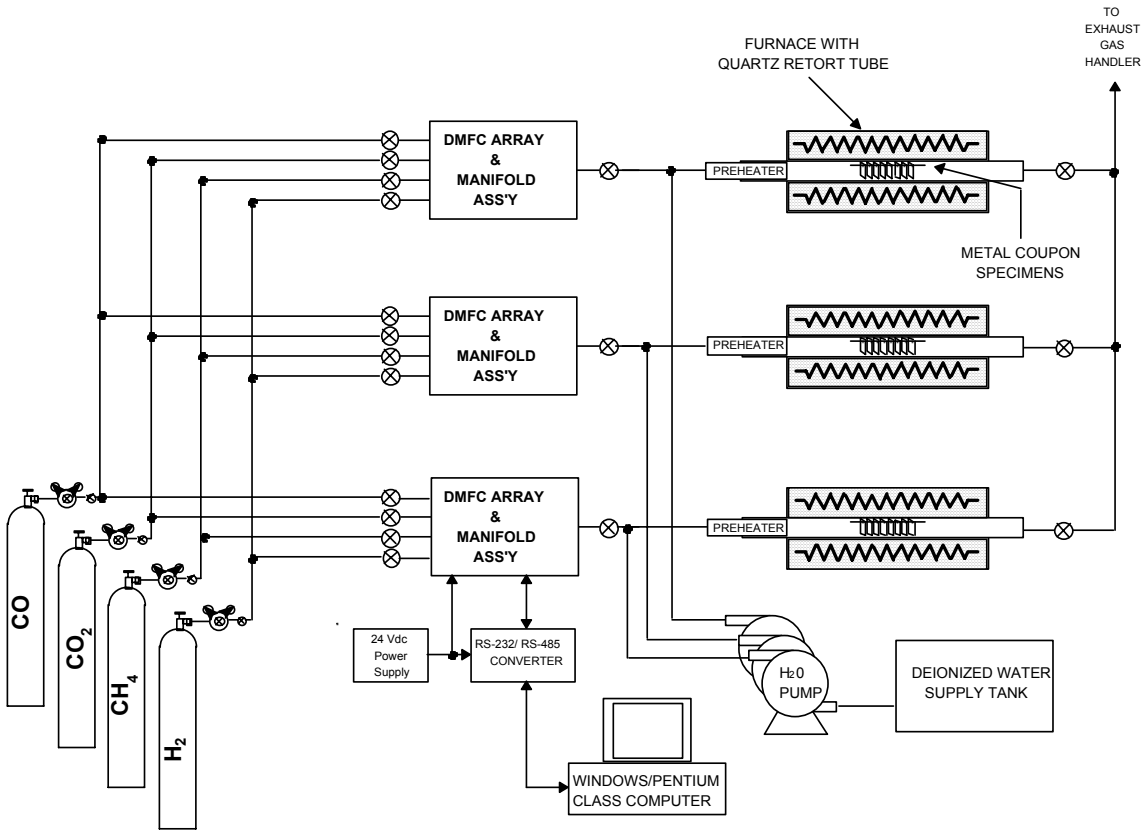

Figure 4 Schematic diagram for three test facilities set up for metal dusting experiments.

The output from each DMFC combined into a central manifold tube that connected to the steam/vapor preheater assembly at the input cover flange for the retort tube. The steam/ vapor preheater had a coaxial-design mixing chamber, enabling the water vapor to be entrained by the flowing gas mixture prior to passing the preheat element. The gas mixture flow rate was typically 200-400 cc/min, and the water flow rate was 1-5 cc/h. Distilled water was supplied to the preheat mixing chamber by a Watson-Marlow Model MPL micro-metering pump that was fed from a 20 L polycarbonate carboy. The micro-metering pump is based on peristaltic action, and the flow rate was adjusted by varying the rotational speed of the roller cam and/or the diameter of the flexible tubing. The gas-steam mixture flowed past the alloy test specimens to the exit port at the rear flange cap. After the gas-steam mixture exited the retort, it was passed through a chilled-water pyrex condenser to collect water vapor while the remaining gas mixture was vented to a room exhaust vent handler. Gas analysis during the exposure tests was provided by a Stanford Research Systems Model QMS100 gas analyzer. Each test system had sampling ports at the inlet of the preheat mixing chamber and at the outlet of the chilled water condenser.

Alloy test specimens were mounted on a quartz specimen tree (see Fig. 5) that was centered in the heat zone of the retort chamber. Metal-dusting experiments were conducted under isothermal conditions at temperatures between 427°C (800°F) and 704°C (1300°F). A chromel-alumel thermocouple controlled the furnace temperature. Specimen temperature was monitored with a second, sheathed chromel-alumel thermocouple inserted into the reaction

chamber in the vicinity of

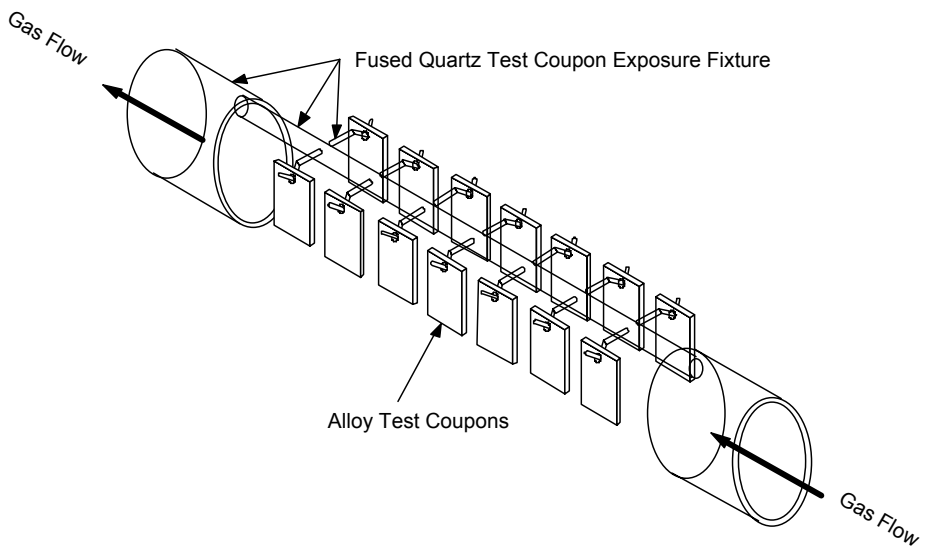

Figure 5 Schematic diagram of quartz specimen holder and test coupon arrangement used for metal dusting experiments.

the specimens. The actual composition of the gas mixture had a wide enough range to establish a_C of ≈0.5 to ≈100 at the temperatures and pressures of interest. The exposure time periods in different experiments ranged between 5 and 1000 h, depending on the objective of the test.

Materials

The test material include a number of Fe- and Ni-base alloys, predominantly those commercially available, selected on the basis of Steering Committee discussions. Table 3 lists the nominal compositions of various alloys selected for evaluation in the program.

The Fe-base alloys included a low-Cr ferritic steel (T22), an intermediate-Cr ferritic steel (T91), and several high-Cr ferritic and austenitic steels and other alloys. The chromium and nickel contents of the high-Cr alloys were in the range of 17.3-26.7 wt.% and 9.3-36.6 wt.%, respectively, except for alloys MA 956 and APMT, which contained no nickel. Several of the Fe-base alloys contained a third element,such as Al or Si, which has a high affinity for O. For example, MA956 and APMT contained 4.5 and 4.9 wt.% Al, respectively. Alloys 153MA, 253MA, and 353MA contained Si in a range of 1.3-1.6 wt.%, whereas Alloy 38815 contained 5.8 wt.% Si.

Generally, the Ni-base alloys had a much more complex chemical composition since they contained Cr (in a range of 15.4-28 wt.%) and several other elements, such as Mo (alloys 617 and 625), Al (601, 617, 602CA, and 214), and Si (45TM and HR 160). Further, several alloys contained Nb, W, and Co, which can also influence their oxidation behavior and their resistance to metal dusting attack.

Surface engineering of select alloys is planned to examine the influence of such treatment on their resistance to metal dusting. The pretreatment involves oxidation of the alloys in an air or a low-pO_2 environment at elevated temperatures. In addition, metallic coatings (primarily enrichment

Table 3 Nominal chemical compositions of alloys selected for the experimental program (wt.%).

Material	C	Cr	Ni	Mn	Si	Mo	Al	Fe	Other
T22	0.20	2.3	–	0.6	0.5	1.0	-	Bal	–
T91	0.08	8.6	0.1	0.5	0.4	1.0	-	Bal	N 0.05, Nb 0.07, V 0.2
153MA	0.05	18.4	9.5	0.6	1.4	0.2	-	Bal	N 0.15, Ce 0.04
253MA	0.09	20.9	10.9	0.6	1.6	0.3	-	Bal	N 0.19, Ce 0.04
353MA	0.05	24.4	34.7	1.4	1.3	0.1	-	Bal	N 0.18, V 0.06
321L	0.02	17.4	9.3	1.8	0.5	-	-	Bal	N 0.02, Ti 0.3
310	0.03	25.5	19.5	1.7	0.7	-	-	Bal	-
800	0.08	20.1	31.7	1.0	0.2	0.3	0.4	Bal	Ti 0.31
803	0.08	25.6	36.6	0.9	0.7	0.2	0.5	34.6	Ti 0.6
38815	0.01	13.9	15.3	0.6	5.8	1.0	0.13	Bal	-
MA956	-	20.0	-	-	-	-	4.5	Bal	Ti 0.5, Y_2O_3 0.6
321	0.04	17.3	10.3	1.2	0.4	-	-	Bal	Ti 0.4, N 0.01
APMT	0.04	21.7	-	0.1	0.6	2.8	4.9	Bal	-
4C54	0.17	26.7	0.3	0.7	0.5	-	-	Bal	N 0.19
									-
600	0.04	15.4	Bal	0.2	0.1	-	-	9.7	-
601	0.03	21.9	61.8	0.2	0.2	0.1	1.4	14.5	Ti 0.3, Nb 0.1
690	0.01	27.2	61.4	0.2	0.1	0.1	0.2	10.2	Ti 0.3
617	0.08	21.6	53.6	0.1	0.1	9.5	1.2	0.9	Co 12.5, Ti 0.3
625	0.05	21.5	Bal	0.3	0.3	9.0	0.2	2.5	Nb 3.7, Ti 0.2
602CA	0.19	25.1	62.6	0.1	0.1	-	2.3	9.3	Ti 0.13, Zr 0.19, Y 0.09
214	0.04	15.9	Bal	0.2	0.1	0.5	3.7	2.5	Zr 0.01, Y 0.006
230	0.11	21.7	60.4	0.5	0.4	1.4	0.3	1.2	W 14, La 0.015
45TM	0.08	27.4	46.4	0.4	2.7	-	-	26.7	RE 0.07
HR 160	0.05	28.0	Bal	0.5	2.8	0.1	0.2	4.0	Co 30.0

RE = rare earth.

of Al or Cr in the surface regions of the alloys) will be applied by a pack diffusion process on several Fe- and Ni-base alloys. Prior to evaluation under metal dusting conditions, the coatings will be oxidized in air at elevated temperatures to develop adherent chromia or alumina scales.

TEST RESULTS AND DISCUSSION

Key Variables for Carbon Deposition and Metal Dusting

Ten short-term runs were conducted to evaluate the role of several variables in the carbon deposition process and in the initiation of metal dusting reactions. The key variables included exposure time, temperature, water content in the exposure gas, and presence/absence of catatytic material during exposure. The range of parameters in the scoping tests included exposure times of 5-100 h, temperatures of 593°C (1100°F) and 704°C (1300°F), gas mixtures with and without H_2O, and presence and absence of catalyzing agent. The specimens included pure Fe, pure Ni, Type 304 stainless steel, Alloys 800 and 601, and Fe aluminide intermetallic.

Runs 2 and 3 were conducted for 100 h at 593°C (1100°F) in Gases 4 and 5, respectively. Gases 4 and 5 had similar composition (see Table 1), except that Gas 5 had 2 vol % H_2O in addition to other gases. The carbon activity values established by the two gases are listed in Table 2. Since Gas 4 contained no H_2O, the a_C values at at 593°C (1100°F), are infinity and 4.98, based on Reactions 1 and 2, respectively. The a_C values for Gas 5 at 593°C (1100°F) are 32.3 and 5.04, based on Reactions 1 and 2, respectively.

In runs 4 and 5, the specimens were exposed to the same two gases at the higher temperature of 704°C (1300°F). The carbon activities established by Gases 4 and 5 at 704°C (1300°F) are infinity and 3.80, based on Reaction 1, whereas the values for both gases would be 0.34, based on Reaction 2. The calculations indicate that, if Reaction 1 determined carbon deposition, a carbon deposit is expected because $a_C > 1$; on the other hand, if Reaction 2 determined the deposition, no deposit of carbon is anticipated because a_C is <1. The observation of significant deposit of carbon in the runs at 704°C (1300°F) indicates that Reaction 1 determines a_C in the exposure environment.

Additional experiments showed that the gas phase reactions, accentuated by the catalytic effect of the metallic specimens consisting of Fe- and Ni-base alloys, lead to $a_C >> 1$, causing a copious amount of carbon deposit even within a short time period of 5 h.

Characteristics of Deposits

Scanning electron microscopy (SEM), Raman spectroscopy, energy dispersive X-ray spectroscopy (EDX), and X-ray diffraction (XRD) have been used to study the microstructure, electron binding, and phase chemistry of the metal dusting products. Graphite has a layered structure with the space group $P6_3/mmc$. Carbon atoms within the layers bond strongly through sp^2 hybridization and arrange in a two-dimensional honeycomb network. The layers are stacked in a hexagonal crystal structure and are bound together by van der Waals force. Because this force is weak, the C-C distance of 335.4 pm between layers is large (Franklin 1951). For this reason, graphite crystals readily disorder along the c-axis (Krebs 1968). The Raman scattering from various forms of carbon is sensitive to the structural disorder of the material (Tuinstra and Koenig 1970; Nakamizo et al. 1977; Nakamizo et al. 1978; Dillon and Woollam 1984). As a result, Raman spectroscopy, a useful nondestructive technique for structural characterization of carbon materials, was used to analyze the characteristics of the carbon that was generated in the metal dusting experiments. Details on the results and analysis are discussed in a companion paper, presented in this workshop (Zeng et al. 2002).

Behavior of Fe- and Ni-base Alloys

Several of the screening tests were used to establish the testing conditions for long-term experiments with Fe- and Ni-base alloys. One of the important results was that the Fe- and Ni-base alloys should not be exposed simultaneously in the same run, since the Fe-base alloys exhibited a carbon deposit much earlier than the Ni-base alloys, and significant cross contamination occurred between these classes of alloys. Even among the Fe-base alloys, the ones with lower Cr contents (e.g., T22) were much more susceptible to carbon deposition and metal dusting attack when exposed under the same conditions of temperature, time, and gas composition.

Several 1000-h experiments were conducted at 482°C (900°F) and 593°C (1100°F) with Fe- and Ni-base alloys in Gas 2 environment, which simulated the chemistry of the reformer

effluent. This gas contained 23 vol.% H_2O, which was achieved by pumping water into the reaction chamber through a specially designed heater.

Detailed analysis of the specimens after exposure at 593°C (1100°F) showed little, if any, deposit of carbon on the specimen surfaces. Carbon was noted primarily on the T22 specimen, and virtually no carbon was detected on Ni-base alloys. The major difference between these runs and

the scoping tests was the amount of H_2O in the exposure environment. Note that a_C established by Gas 2 at 593°C (1100°F) is $\geq$2 (see Table 2), yet no deposit of carbon was noted, even after 1000 h of exposure.

Another experiment was conducted to examine the competing effects of oxidation and carbon deposition/metal dusting on alloy behavior. In this experiment, Fe-base alloys were exposed in Gas 2, but with only 2 vol.% H_2O, instead of the 23 vol.% tested earlier. The calculated values for a_C in experiments at 593°C (1100°F) with 23 and 2 vol.% H_2O were 2 and 30, respectively. In the experiment with low H_2O, a copious amount of carbon was observed on specimen surfaces. Figure 6 shows a macroscopic photograph of the specimens exposed in the two experiments.

Detailed analysis of the surfaces of specimens exposed in the gas environment containing 23 vol.% H_2O indicated development of oxide layers on most of the specimens. Figures 7-9 show SEM photomicrographs of surfaces of several Fe-base alloys after 1000-h exposure at 593°C (1100°F). In general, most of the alloys exhibited oxide scales on the surface; however, at isolated locations some carbon deposit adhered to the surface. No significant pitting-type attack was noted in any of the high-Cr specimens. The only alloy that exhibited a copious amount of carbon deposit

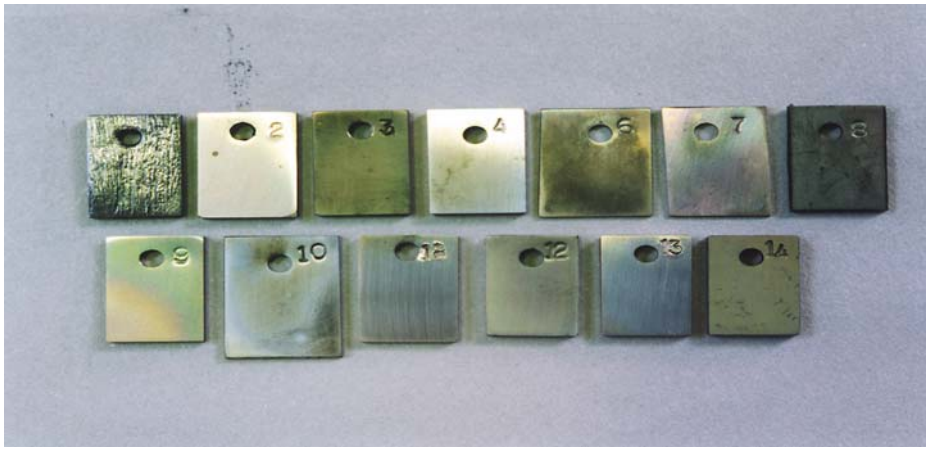

Figure 6 Macrophotographs of Fe-base alloy specimens after 1000-h exposure at 593°C (1100°F) in (top) Gas 2 with 23.1 vol.% H_2O and (bottom) Gas 2 with 2 vol.% H_2O.

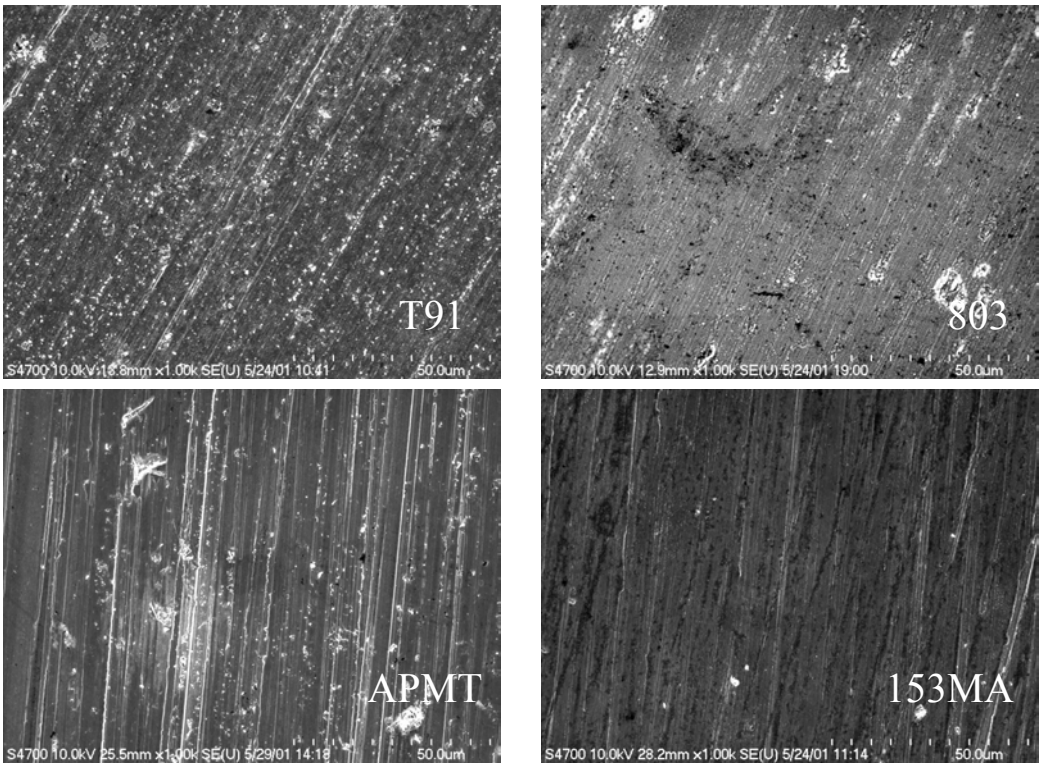

Figure 7 SEM photomicrographs of surfaces of (top left) T91, (top right) 803, (bottom left) APMT, and (bottom right) 153MA after 1000 h exposure in Gas 2 environment.

and metal dusting was T22 steel, which contained 2.25 wt.% Cr. EDX analysis showed that MA956 and APMT (which contained 4.5 and 4.9 wt.% Al, respectively) developed thin alumina scales, whereas 253MA and 38815 (even though they contained 1.6 and 5.8 wt.% Si, respectively) only developed chromia or (Fe,Cr) oxide scales.

Figures 10 and 11 show SEM photomicrographs of surfaces of several Ni-base alloys after 1000-h exposure in Gas 2 environment at 593°C (1100°F). In general, Ni-base alloys develop

much thinner oxide scales than the Fe-base alloys. However, carbon adherence onto the surface of Ni-base alloy is much stronger, as evidenced by the presence of it even after prolonged ultrasonic cleaning. Furthermore, the carbon deposit can be seen as striations, forming preferentially along the polishing lines on the surface and in a nonuniform distribution.

To examine carbon penetration, if any, into the alloys, several of the exposed specimens were cut, mounted, polished, and cross sectioned for SEM and EDX. Figures 12 and 13 show the SEM photomicrographs of cross sections of several Fe- and Ni-base alloys, respectively, after 1000-h exposure in the metal dusting environment. T91 alloy developed a thin oxide scale and virtually no carbon penetration, even after 1000-h exposure. The oxide scale developed on Alloy 800 was porous and discontinuous, and several pits initiated from the surface (see Fig. 12). Alloy 321 developed a thin oxide scale with almost no carbon penetration into the alloy, indicating that the spots of carbon observed on the surface (see Fig. 8) are primarily adherent to the thin oxide layer.

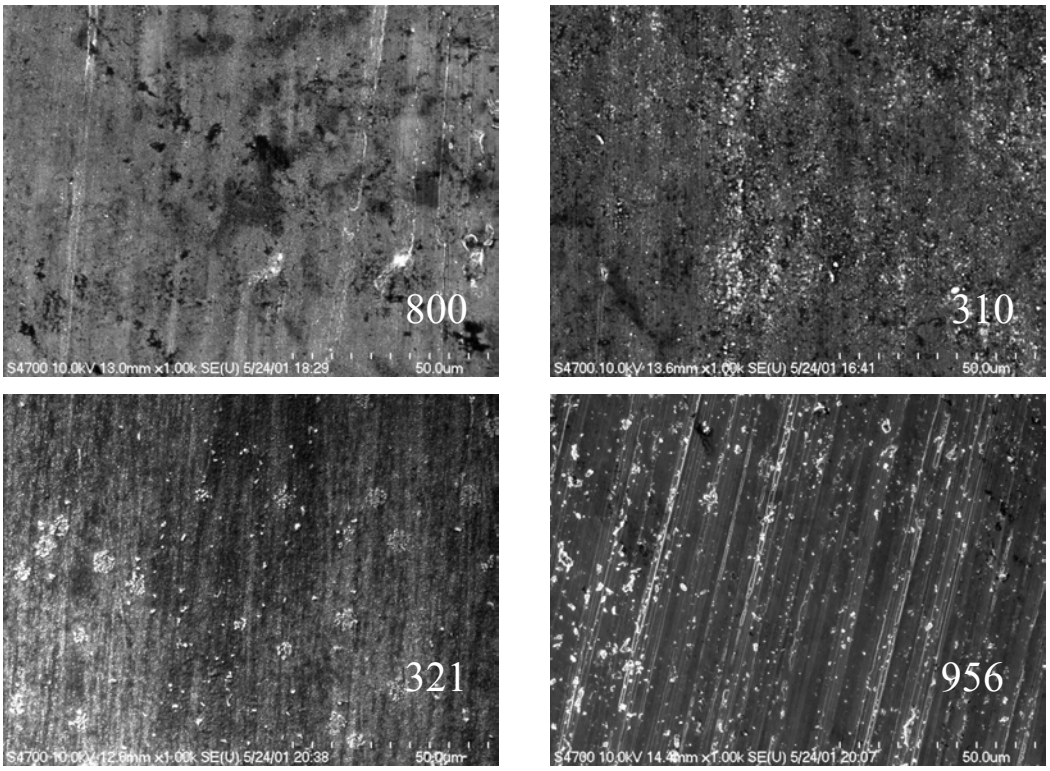

Figure 8 SEM photomicrographs of surfaces of (top left) Alloy 800, (top right) 310 SS, (bottom left) 321 SS, and (bottom right) MA956 after 1000-h exposure in Gas 2 environment.

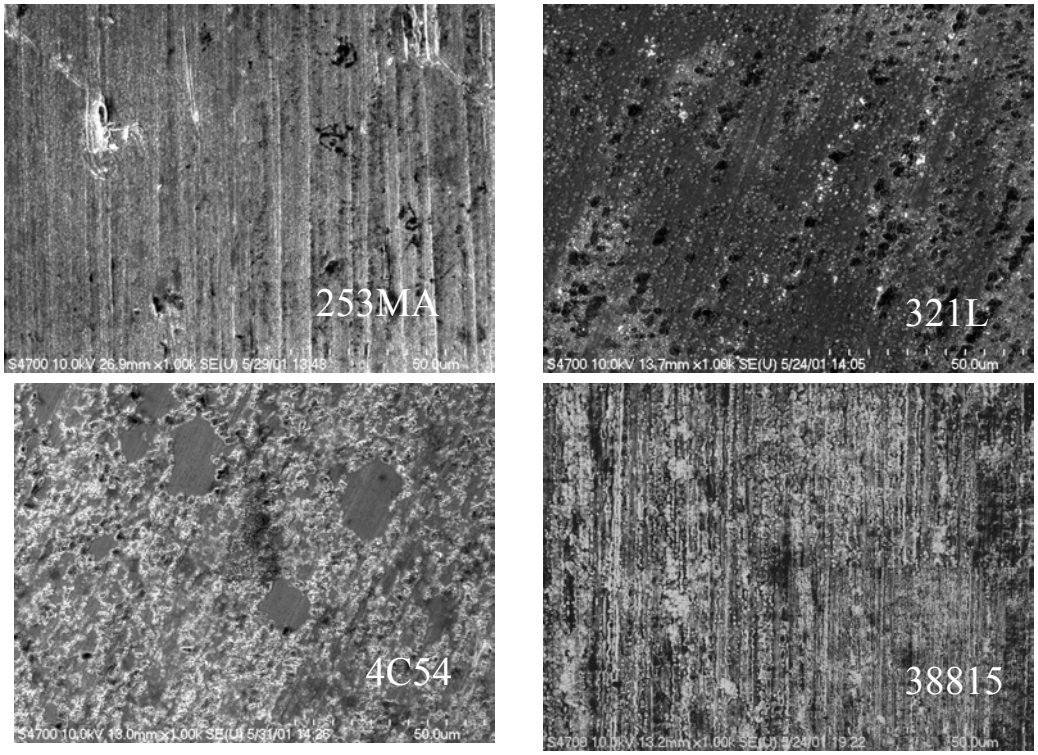

Figure 9 SEM photomicrographs of surfaces of (top left) 253MA, (top right) 321L, (bottom left) 4C54, and (bottom right) 38815 after 1000-h exposure in Gas 2 environment.

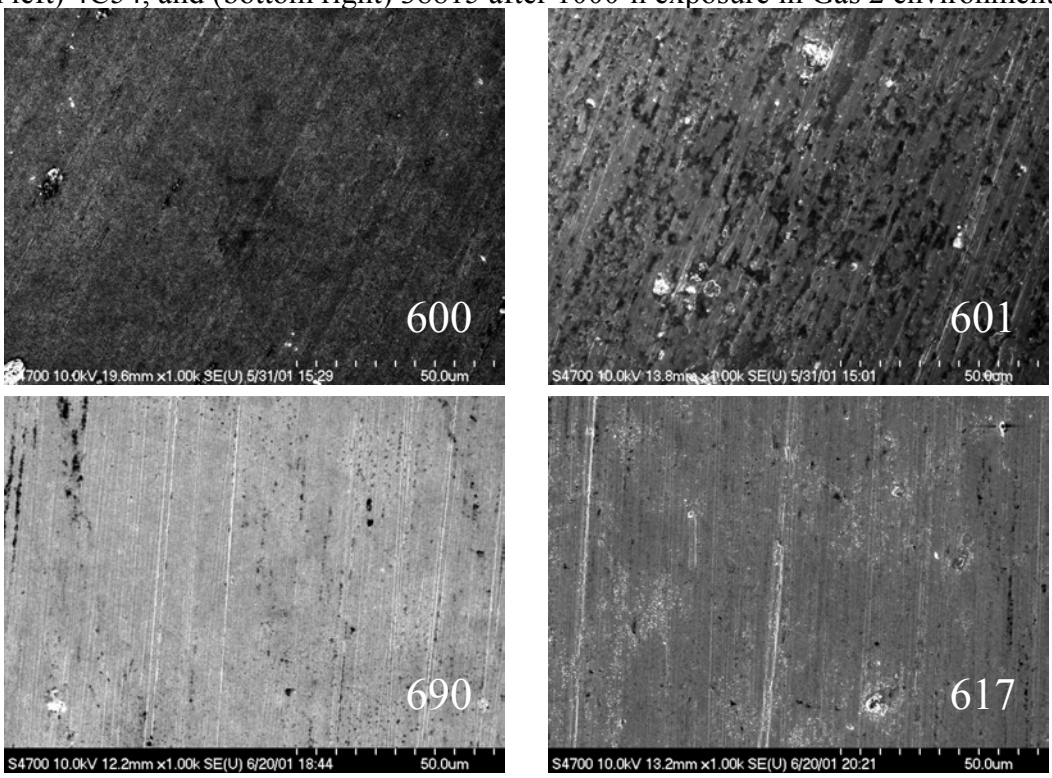

Figure 10 SEM photomicrographs of surfaces of (top left) 600, (top right) 601, (bottom left) 690, and (bottom right) 617 after 1000-h exposure in Gas 2 environment.

Among the Ni-base alloys, 600, 690, 602CA, and 45TM were examined in cross section. Figure 13 shows the SEM photomicrographs of these specimens. The scales were continuous and adherent to the substrate, and the thickness was 0.1-0.2 μm after 1000-h exposure in Gas 2 at 593°C (1100°F). None of the alloys exhibited internal penetration of carbon or pitting attack.

Raman spectroscopy was used to analyze the carbon that adhered to the surface on Fe- and Ni-base alloys exposed in Gas 2 environment at 593°C (1100°F). Figure 14 shows Raman spectra (frequency range 1200-1700 cm^{-1}) for carbon that adhered to the surface of alloys T22, T91, 153MA, and 253MA (which had Cr contents of 2.25, 8.6, 18.4, and 20.9, respectively). The alloy T22, which exhibited severe metal dusting attack, had much sharper peaks for carbon when compared with those for the other alloys. Figure 15 shows the Raman spectra (frequency range 200-800 cm^{-1}) obtained on the surfaces of several Fe-base alloys with different Cr contents, after 1000-h exposure. The Raman spectra in the frequency range 200-800 cm^{-1} clearly show that alloys with Cr >8.6 wt.% develop oxide scales, as evidenced by the SEM photomicrographs presented earlier. The peaks at ≈550 and ≈680 cm^{-1} correspond to Cr_2O_3 and (Fe,Cr) oxide spinel, respectively. Lack of oxide scale on alloy T22 (which contained 2.3 wt.% Cr) led to metal dusting attack during the 1000-h exposure.

Figure 16 shows the Raman spectra (frequency range 200-800 cm^{-1}) for three Ni-base alloys with different Cr contents after 1000-h exposure in the metal dusting environment at 593°C (1100°F). The alloys predominantly developed Cr_2O_3, as indicated by the peak at ≈550 cm^{-1}. The peak height seems to be strongly dependent on the Cr content of the alloy; for example, among the

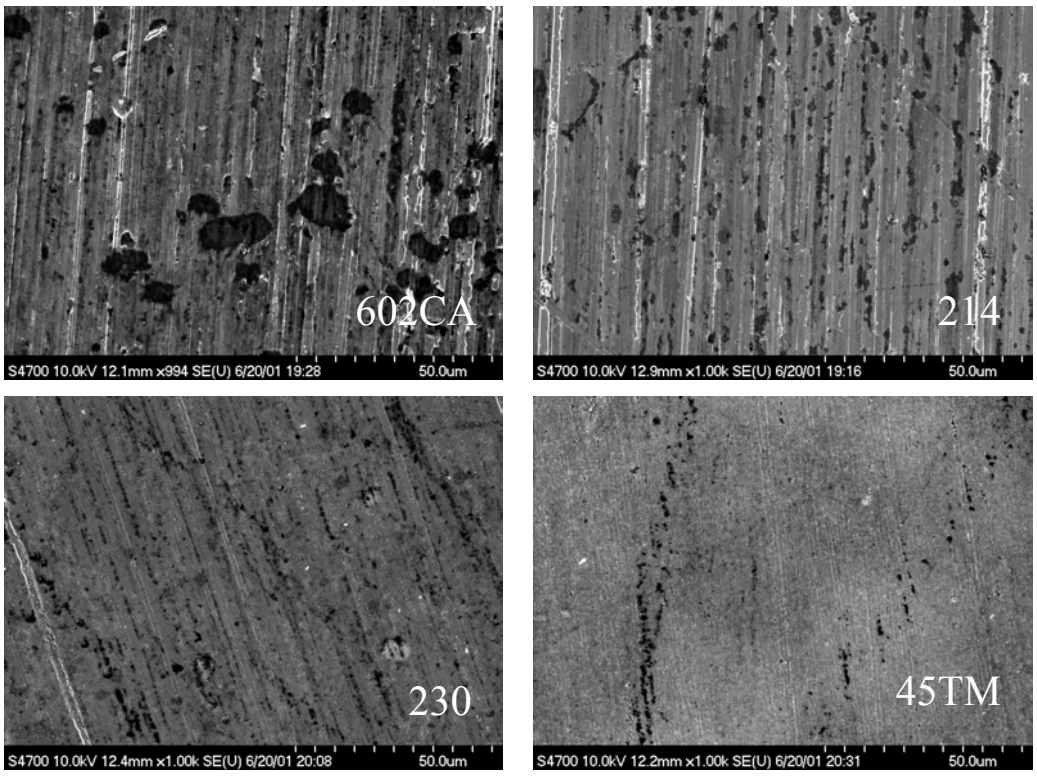

Figure 11 SEM photomicrographs of surfaces of (top left) 602CA, (top right) 214, (bottom left) 230, and (bottom right) 45TM after 1000-h exposure in Gas 2 environment.

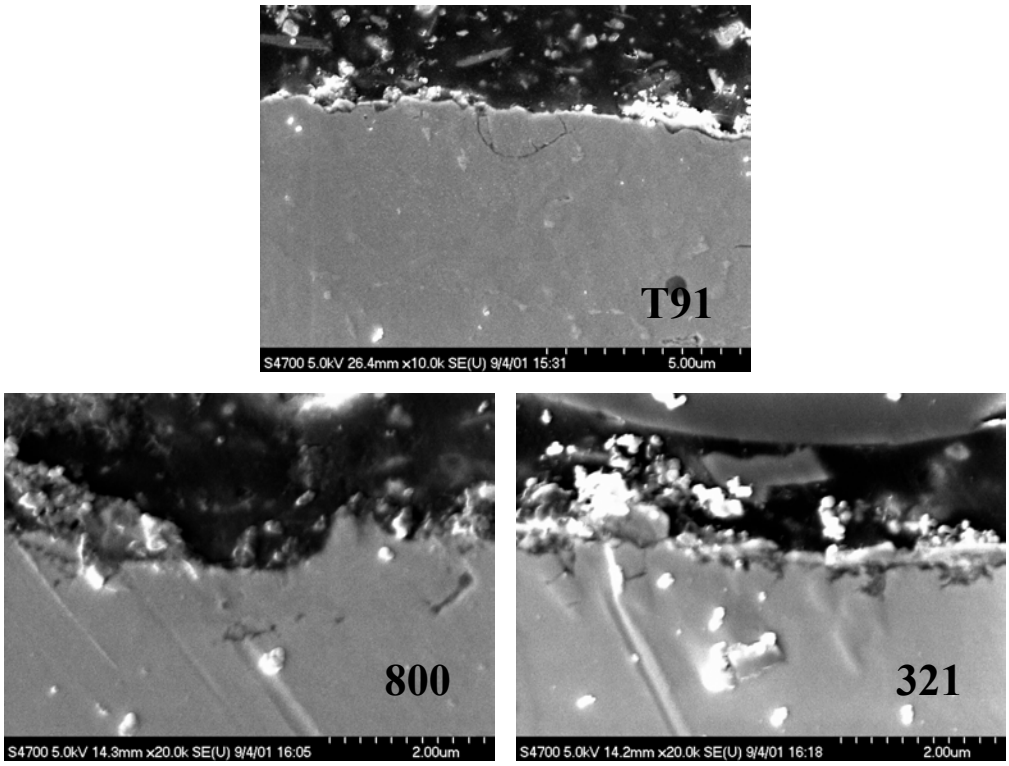

Figure 12 SEM photomicrographs of cross sections of (top) T91, (bottom left) 800, and (bottom right) 321 after 1000-h exposure in Gas 2 environment.

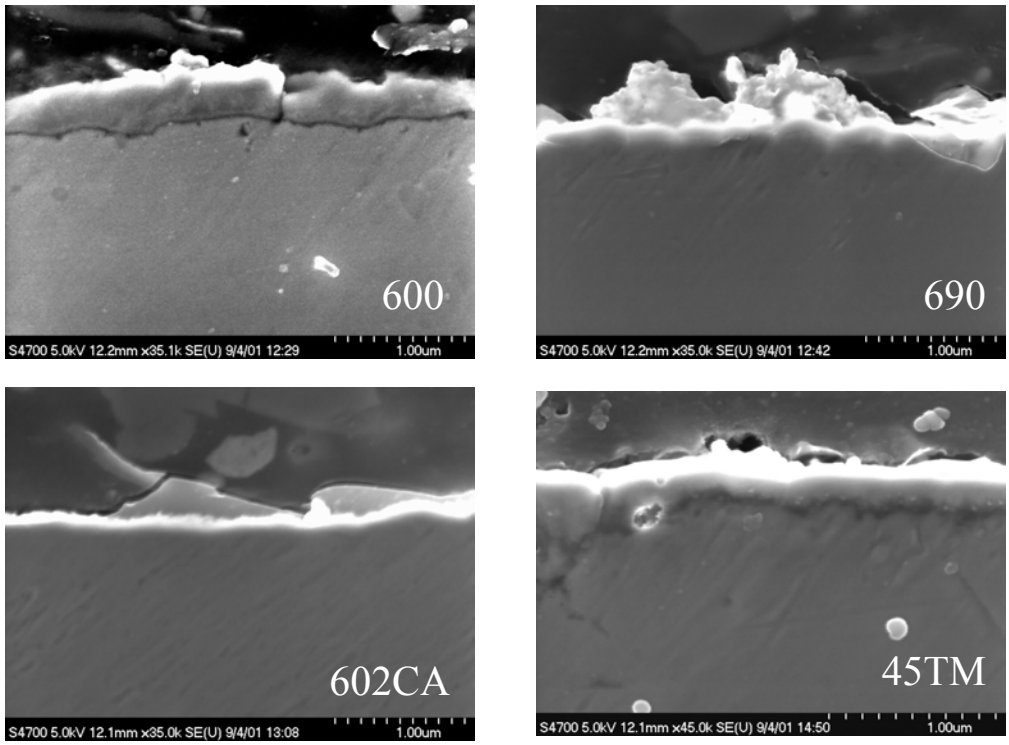

Figure 13 SEM photomicrographs of cross sections of (top left) 600, (top right) 690, (bottom left) 602CA, and (bottom right) 45TM after 1000-h exposure in Gas 2 environment.

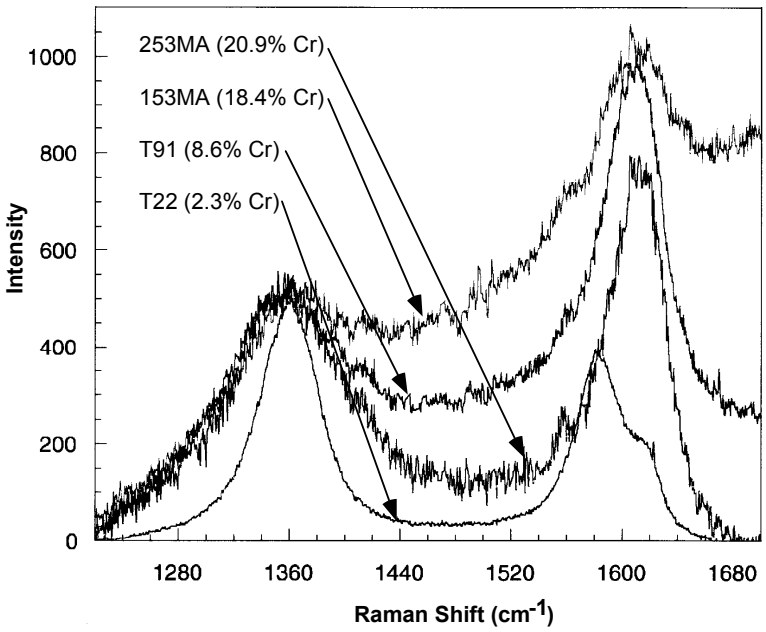

Figure 14 Raman spectra for carbon adhered to several alloys with different Cr contents after 1000-h exposure in Gas 2 environment at 593°C (1100°F).

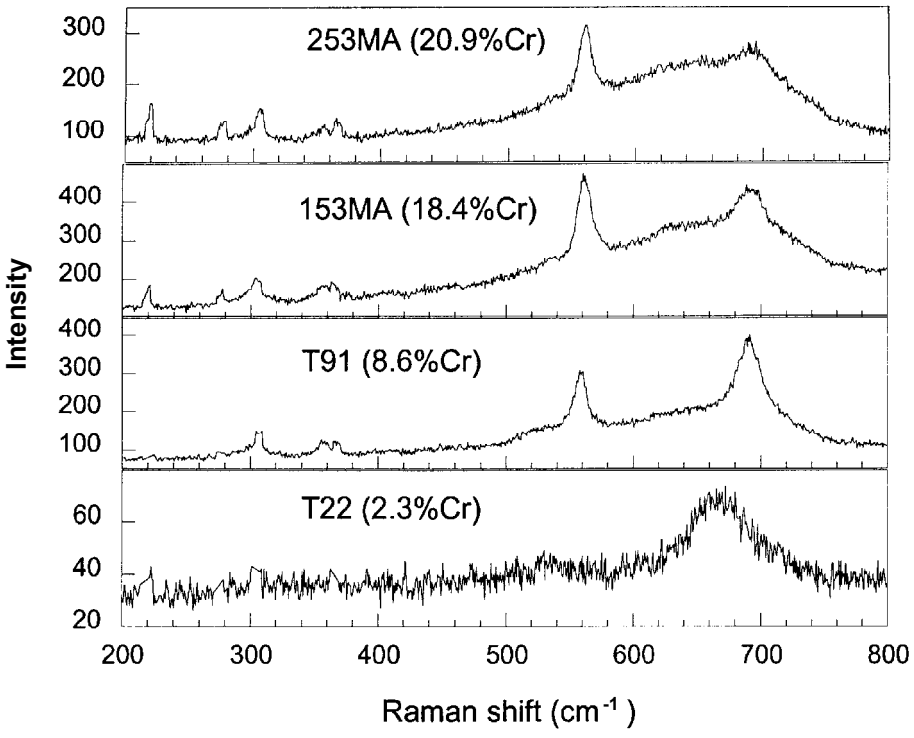

Figure 15 Raman spectra for surfaces of several Fe-base alloys with different Cr contents after 1000-h exposure in Gas 2 environment at 593°C (1100°F).

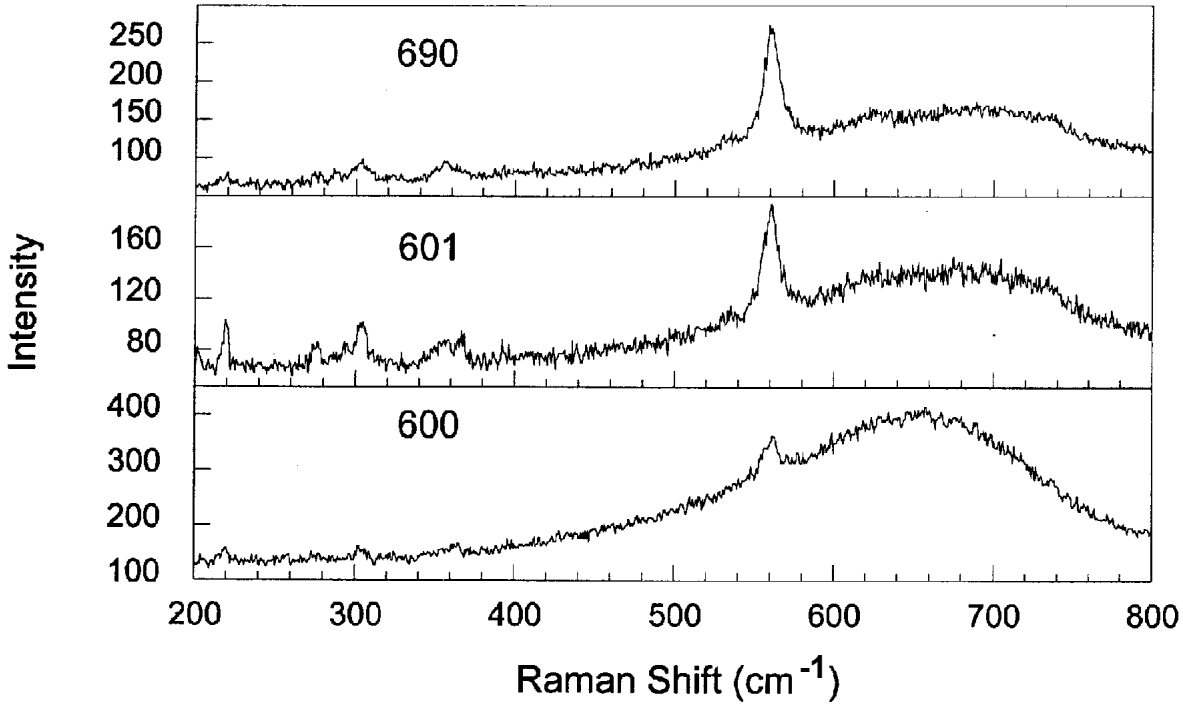

Figure 16 Raman spectra for surfaces of several Ni-base alloys with different Cr content after 1000-h exposure in Gas 2 environment at 593°C (1100°F).

three alloys, the peak height is smallest for Alloy 600 (15.4 wt.% Cr) and largest for Alloy 690 (27.2 wt.% Cr). The broad feature in these spectra at ≈660 cm^{-1} is not currently identified but seems to disappear as the Cr level in the alloy increases.

Raman analysis was also performed on several alloys that had deliberate additions of Al.[10] Even though the Al content of alloys MA956 and APMT is similar, their scaling behavior is somewhat different. Alloy APMT predominantly developed Cr_2O_3 scale, as evidenced by a sharp peak at ≈550 cm^{-1}, whereas the alloy MA956 (which exhibited a much thinner scale) showed a less developed peak at a frequency >550 cm^{-1}. A peak at ≈700 cm^{-1} was observed in the APMT alloy; this peak is not presently identified, but it does not correspond to any of the Al_2O_3 phases. Even in the higher frequency range (corresponding to carbon), the relative intensities for the D-to-G band for the two alloys are different, but the cause is not known. The Raman spectra for the alloys 602CA and 214 (with a lower Al content) were similar in the entire frequency range.

Raman analysis was also performed on several alloys that had deliberate additions of Si.[10] The alloys selected for comparison included 253MA, 38815, 45TM, and HR160, which contain 13.9-28.0 wt.% Cr and 1.6-5.8 wt.% Si, respectively. The results showed that all four alloys developed predominantly Cr_2O_3 scale, which is expected based on oxidation studies of Si-containing alloys. In general, Si can form a silica scale at the Cr_2O_3/alloy interface since the diffusion coefficient for Si is much smaller than that for either Cr or Fe, and these alloys can rarely form an external scale of silica at the concentration levels present. The Raman spectra in the frequency range of 1200-1800 cm^{-1} showed similar peaks on all four alloys, indicating that the variation in Si content had virtually no effect on the carbon deposition.

Initiation of Metal Dusting

The results presented thus far clearly indicate that the gas chemistry used (simulating reformer effluent) in our study can deposit carbon by the two reactions discussed earlier. Furthermore, decreasing the H_2O content (e.g., from 23 to 2.0 vol.%) in the gas can increase a_C, thereby accelerating carbon deposition. However, whether the deposited carbon can initiate metal dusting in Fe- and Ni-base alloys is strongly influenced by the oxidation characteristics of the alloys. The competition between the oxidation process to form a continuous oxide scale on a given alloy surface and deposition and penetration of carbon will determine the incubation time for metal dusting attack to occur. If an alloy can develop a protective oxide scale fast enough and early during exposure, then subsequent deposition of carbon on top of the oxide layer can delay initiation of metal dusting.

In most earlier studies on metal dusting, the researchers selected gas compositions that yielded carbon activities >>1, which led to deposition of carbon on the specimens from the beginning of the exposure (Grabke 1998; Maier et al. 1998; Baker and Smith 2001; Levi et al. 2001). Besides exposure to high carbon activity, the alloys did not have much time (before carbon deposition) to develop a protective oxide scale. Therefore, the earlier studies emphasized interaction of the deposited carbon with the constituents of the structural alloys and examined the role of alloy-related variables (such as alloy composition; Fe, Cr, and Ni contents; surface preparation; and surface roughness) on alloy degradation. A comparative analysis was conducted on the carbon activities and oxygen partial pressures established in several studies to better understand the role of gas chemistry in the metal dusting behavior of structural alloys.

Table 4 lists the chemical compositions of gases used in several of the studies. The H_2O content in the past studies was in the range of 0-2.4 vol.%, whereas in the present studies, we used H_2O contents of 0, 2, and 23 vol.% (the last one is typical of the effluent from a H_2 reformer). Similar to results presented in an earlier section, we calculated a_C for the gas mixtures (used in earlier studies) at several temperatures in the range of 425-760°C (800-1400°F).

Table 5 lists the carbon activity values at 593°C (1100°F) calculated for gas mixtures used in past studies and the current program. The calculations are based on whether Reaction 1 or 2 was dominant or equilibrium between different gas species prevailed at the elevated temperature. The carbon activities in past studies have been >>1, irrespective of whether Reaction 1 or 2 dominated the process. If the gases were in thermodynamic equilibrium, the carbon activity in most cases is around 1. A carbon activity value of infinity under the Reaction 1 column (in Table 5) arises because the inlet gas mixture in the study did not contain H_2O, whereas infinity under Reaction 2 arises because the mixture did not contain CO_2. The calculated carbon activity values are based on initial gas compositions. Once Reaction 1 starts, H_2O will be generated, and the local carbon activity will be less than the calculated values in Table 5. However, carbon deposition would have occurred, and it would be almost impossible to develop a protective oxide scale on the alloy surface.

Table 4 Gas chemistries used in metal dusting research.

	Composition in vol.%				
Researcher	**CO**	**CO_2**	**CH_4**	**H_2**	**H_2O**
Grabke	24.7	-	-	73.4	1.9
Maier et al.	24.4	-	-	73.2	2.4
Baker/Smith	70.0	4.0	-	25.3	0.75
Levi et al.	25.0	-	-	75.0	-
Natesan et al. (gas 4)	17.5	8.3	-	74.2	-
Natesan et al. (gas 5)	17.6	8.3	-	72.2	2.0
Natesan et al. (gas 2)	18.0	5.6	1.1	52.0	23.0

Table 5 Carbon activity and oxygen partial pressure values at 593°C (1100°F), calculated for gas mixtures used by various researchers.

	Carbon activity			Oxygen pressure (in atm), based on		
Researcher	**Rxn 1**	**Rxn 2**	**Eqm**	**CO/CO_2**	**H_2/H_2O**	**Eqm**
Grabke	47.5	∞	1.2	-	6.7×10^{-28}	7.6×10^{-26}
Maier et al.	37.1	∞	1.2	-	1.1×10^{-27}	7.7×10^{-26}
Baker/Smith	118.0	165.0	0.8	3.1×10^{-28}	1.0×10^{-28}	3.9×10^{-25}
Levi et al.	∞	∞	1.2	-	-	6.9×10^{-26}
Natesan et al. (gas 4)	∞	5.0	1.3	2.2×10^{-26}	-	1.1×10^{-25}
Natesan et al. (gas 5)	32.5	5.0	1.2	2.2×10^{-26}	7.6×10^{-28}	1.2×10^{-25}
Natesan et al. (gas 2)	2.0	7.9	0.7	9.5×10^{-27}	1.2×10^{-25}	2.4×10^{-25}

Table 5 also lists the pO_2 values at 593°C (1100°F), calculated for three possible assumptions: (1 and 2) CO/CO_2 or H_2/H_2O ratio determines the pO_2, or (3) thermodynamic equilibrium exists among all the gaseous species at the elevated temperature. The calculations indicate that for a given gas composition, the equilibrium pO_2 values are always higher than those established by either CO/CO_2 or H_2/H_2O ratios. If one assumes that the gas composition does not change significantly during flow from the exit of the reformer to low-temperature sections of the waste-heat boiler (i.e., the carbon deposition reactions are slow enough that the generation of carbon by catalysis of gas-phase constituents causes little change in bulk gas chemistry), then the pO_2 in the environment will be dictated by the higher of the two values calculated from the CO/CO_2 and H_2/H_2O ratios.

From the materials standpoint, one can analyze the type of interactions between the constituents of the alloy and the environment by means of thermochemical diagrams. Since carbon deposition and formation of the oxide layer on the metal surface are of interest for materials exposed to metal dusting environments, oxygen/carbon diagrams were generated for several temperatures in the range of 400-700°C. Figure 17 shows the oxygen/carbon thermochemical diagrams for Fe, Cr, and Ni calculated for 593°C (1100°F). The diagrams depict the stability fields for the metals, oxides, and carbides of Fe, Cr, and Ni in terms of carbon and oxygen partial pressures. Superimposed on these diagrams (indicated by boxes) are the oxygen and carbon partial pressure ranges for gas mixtures used by various researchers in metal dusting studies. The calculations show that Fe_3C, Cr_2O_3, Ni, and Ni_3C are the phases that will be stable in the environments used in the laboratory research and in gas mixtures corresponding to the effluent of the H_2 reformer (Gas 2).

For pure Fe and for Fe-base alloys containing low concentrations of Cr (e.g., T22), the calculations indicate that Fe_3C would be the primary phase that forms upon exposure to the metal dusting environment. In the case of Fe- and Ni-base alloys containing high Cr concentration, pure Cr oxide or Cr-rich oxide will be the stable phase that forms upon exposure of the alloy to metal dusting environments, unless precipitous deposition of carbon occurs from the beginning of exposure such that the alloy surface is completely covered with carbon and no time is available to develop an oxide scale. We believe such was the case in most of the earlier studies, which had $a_C >> 1$ and extremely low H_2O content. In the study conducted at ANL, the H_2O content of Gas Mixture 2 was 23 vol.%, and a_C was somewhat greater than 1. For this condition, the alloys exhibited oxide scales with subsequent deposition of carbon on top of the oxide.

In reformers, the metal dusting attack generally occurs over a period of years of service, while in laboratory studies the attack occurs over a period of a few hours to few days. Thus, in the reformer, the degradation process is dictated by the breakdown of the oxide scale, while in the laboratory studies, attack begins right from the start. The ongoing program at ANL will examine the competition between the oxide scale development and its breakdown leading to metal dusting attack. Therefore, an understanding of the incubation period and initiation time for development of metal dusting morphology (such as surface pits) will be emphasized, in addition to evaluation of the role(s) of alloy chemistry and surface modification in mitigating metal dusting degradation.

SUMMARY

The deposition of carbon from cabonaceous gaseous environments is prevalent in many chemical and petrochemical processes such as reforming systems, syngas production systems, iron reduction plants, and others. One of the major consequences of carbon deposition is the

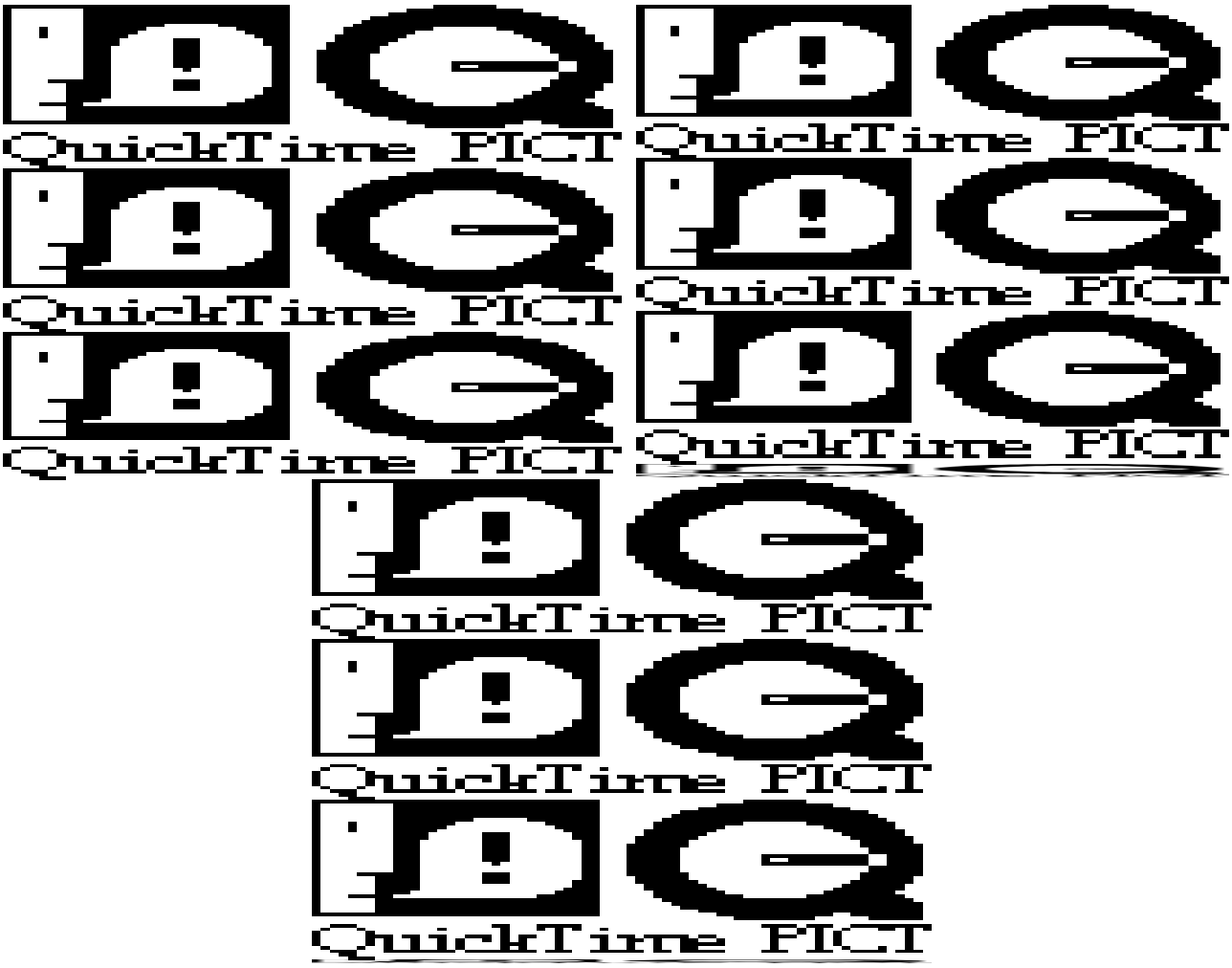

Figure 17 Oxygen/carbon thermochemical diagrams for Fe, Cr, and Ni calculated for 593°C (1100°F).

degradation of structural materials by a phenomenon known as "metal dusting." There are two major issues of importance in metal dusting. First is formation of carbon and subsequent deposition of carbon on metallic materials. Second is the initiation of metal dusting degradation of the alloy. The first is influenced by a_C in the gas mixture and availability of the catalytic surface for carbon-producing reactions to proceed. There may be a threshold in a_C (>>1) for carbon deposition. Metal dusting of the alloy in the reformer environments is determined by a competition between the oxide scale development and access of the virgin metal surface to the carbon deposit. The presence of an oxide scale may not prevent metal dusting but can delay its initiation, thereby slowing the overall attack.

The local nature of dusting (initiated by pits on the alloy surface) on both Fe- and Ni-base alloys shows that defects in the oxide scales play a large role in initiation. Oxide scaling may not occur if a_C is >>1 and/or if the H_2O content in the environment is very low. Laboratory

experiments have clearly indicated the effect of gas chemistry (in particular H_2O content) in the scaling, carbon deposition, and dusting initiation. It is evident that the environment in reformers is high enough in pO_2 that a Cr-rich alloy will develop a chromia scale (given enough exposure time) before carbon deposition.

REFERENCES

Baker, B. and G. D. Smith, 2001, NACE Corrosion 2001, Paper # 01375.

Camp, E. Q., C. Phillips, and L. Gross, 1945, Corrosion, 1, 149.

Dillon, R. O. and J. A. Woollam, 1984, Physical Review B, 29, 3482.

Franklin, R. E., 1951, Acta Cryst., 4, 253.

Grabke, H. J., Materials and Corrosion, 1998, 49, 303.

Hoyt, W. B., R. H. Caughey, 1959, Corrosion, 15, 627.

Krebs, H., 1968, Fundamentals of Inorganic Crystal Chemistry, McGraw-Hill, p. 150.

Levi, T. P., N. Briggs, I. Minchington, and C. W. Thomas, 2001, NACE Corrosion 2001, Paper # 01375.

Maier, M., J. F. Norton, and P. D. Frampton, 1998, Materials and Corrosion, 49, 330-335.

Nakamizo, M., H. Honda, M. Inagaki, and Y. Hishiyama, 1977, Carbon, 15, 295.

Nakamizo, M., H. Honda, and M. Inagaki, 1978, Carbon, 16, 281.

Tuinstra, F. and J. L. Koenig, J. Chem. Phy. 1970, 53, 1126.

Zeng, Z., K. Natesan, and V. Maroni, this workshop proceedings.

ACKNOWLEDGMENTS

This work was sponsored by the U.S. Department of Energy, Office of Industrial Technologies, and Dr. Charles Sorrell was the Program Manager for the project. Specimens of various alloys were supplied by Haynes International, AvestaPolarit, Sandvik Steel, Special Metals, Allegheny Ludlum, and Krupp VDM.